Direct Numerical Simulations of Turbulence

Data Generation and Statistical Analysis

Susan Kurien and Mark A. Taylor

In 1941, Andrei N. Kolmogorov predicted that, within all highly turbulent flows, there is a universal energy-conserving cascade whereby the energy of the large-scale eddies is transferred to finer and finer scales, down to the scales at which the energy is finally dissipated to heat. It is difficult to measure such a cascade directly, but related benchmark predictions for the statistical behavior of turbulent flows can now be calculated and examined using advanced simulation and flow visualization tools. Los Alamos scientists have been able to simulate flows of Reynolds numbers up to 10^5, the largest of which needed of the order of terabytes of data storage and used the full power of the Advanced Simulation and Computing (ASC) Q machine for several weeks of computer time. Through clever analysis of single frames of the simulations, a great deal of information can be extracted to show that the original constraints for the Kolmogorov theory can be relaxed so that, in fact, his statistical predictions hold locally in time. Furthermore, scientists are able to measure new statistical quantities that demonstrate the conditions under which departures from Kolmogorov theory begin to occur. This type of statistical analysis of numerical data is setting the agenda for future research.

Visualization of vorticity in a portion of a 256^3 subdomain of the 2048^3 turbulence simulation performed on the ASC Q machine at Los Alamos.

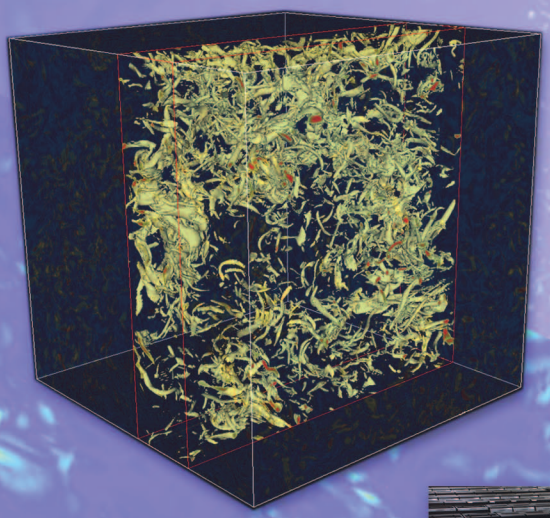

The ASC Q machine.

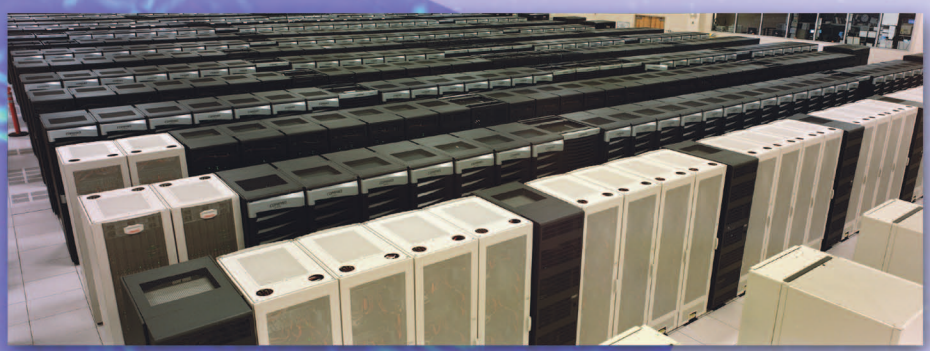

The problem of fluid turbulence has benefited from concerted efforts in theoretical, experimental, and most recently, computational research. However, while theoretical and experimental efforts have cooperated for some time to advance the field, computational science is a relatively recent entry and provides new data and problems that have not been accessible by more established techniques. For some problems, the entire turbulent flow field can now be calculated to high precision with suitable numerical methods. Flow visualization and extensive three-dimensional (3-D) statistical analysis, for example, are techniques that can be used profitably. Computational capabilities and expertise at Los Alamos National Laboratory have resulted in calculations that reveal new universal properties of turbulence and new directions in which to expand research efforts, as we describe below.

Solving the Navier-Stokes equations, which provide the best-known mathematical description of turbulent flow, remains an immensely challenging problem. However, turbulence research is driven by a practical need for real-world engineering applications and by the need to understand and predict the universal fundamental features, if any, in all turbulent phenomena. Therefore, approaches to studying turbulence other than computational ones have evolved over several decades and have produced a deep understanding of the subject on a fundamental as well as a phenomenological level. One such approach was initiated in the late 19th century by Osborne Reynolds, who proposed to ignore the details of the turbulent flow at each instant and, instead, to regard the flow as a superposition of mean and fluctuating parts. What naturally followed this shift in approach was the addition of statistics and probability theory to the arsenal of tools used to understand turbulence. The turbulence field is considered to be a random field in the probabilistic sense. The idea is to study the statistical moments of turbulent fields such as the multipoint correlation functions of velocity, pressure, and so on with the aim to recover the full probability-distribution function of the field and its evolution given a set of initial (boundary) conditions. Alternatively, there are attempts to obtain the probability distribution functions first and derive from them the statistics of the turbulent system. In a broad sense, deriving these functions is the goal of statistical hydrodynamics research (refer to the article " Field Theory and Statistical Hydrodynamics" on page 181 of this volume). This article will examine some of the questions that statistical analysis of turbulence data can address using several data sets generated by solving the Navier-Stokes equations on grids with different spatial resolutions.

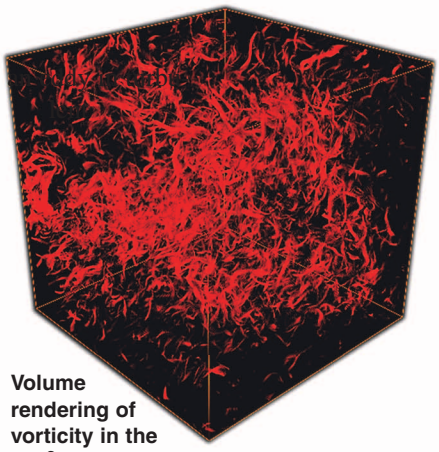

Volume rendering of vorticity in the 256^3 subdomain shown on the opposite page.

Universal Properties of Turbulence

First, we briefly address the problem of universality of statistical properties. We would like to know whether turbulence exists independently of the type of flow (water flowing in a pipe or in a river, wind flow, and others), the fluid that is flowing (air or water), the boundary conditions (smooth, rough, artificial, or periodic), or the energy-input mechanisms (stirring, shaking, or shearing). Is there a regime of length scales that has quantifiable properties common to all turbulent flows? Two phenomenological ideas have been useful in addressing this question. The first was proposed by Lewis F. Richardson in the late 19th century and is consistent with our intuition from observing turbulence—the energy input at large scales is transferred into successively smaller eddies of the turbulent flow in a so-called cascade process. The notion of an "eddy" in turbulent flow is somewhat nebulous, but for current purposes, it should be thought of as a coherent turbulence structure with an associated length scale, location, and lifetime. The second idea is a hypothesis advanced by Andrei N. Kolmogorov (1941): For highly turbulent flows in which the Richardson cascade has created many generations of eddies, the turbulent length scales of size r that are much smaller than the typical large scale L of the flow and much larger than the viscous dissipative scale η must have universal statistical properties. Kolmogorov conjectured that, in this regime of intermediate scales, the dynamics is minimally affected by forcing, boundaries, and large-scale anisotropies, which are generally flow-dependent, and unaffected by the viscous dissipative effects that occur at the very small scales. The dynamics in this so-called inertial range are dominated by the nonlinear term of the Navier-Stokes equations, and it seems reasonable that inertial-range dynamics should display universal behavior statistically. In our discussion of new statistical-analysis and diagnostic techniques, we will be concerned primarily with the statistics of this universal inertial range of scales in high-Reynolds-number turbulence (see the article " The Turbulence Problem" on page 124

for definitions of these terms).

The typical statistical scale-dependent quantities investigated are known as structure functions, one type of which is

$$S_n(r) = \left\langle \left[u_L(\mathbf{x}+\mathbf{r}) - u_L(\mathbf{x}) \right]^n \right\rangle , \quad (1)$$

where $u_L(x) = \mathbf{u}(x)\cdot\hat{\mathbf{r}}$ is the component of the velocity along $\mathbf{r}$ (the subscript L denotes longitudinal velocity) and $\langle ... \rangle$ denotes ensemble and domain averaging over all $\mathbf{x}$. This structure function is thus the nth-order moment of the velocity difference across scales of size r and is a measure, order by order, of the statistical properties of eddies of size r. Kolmogorov derived a fundamental physical law for the inertial range of scales r for high Reynolds number, slowly decaying (essentially steady-state) turbulence under the assumption of isotropy and homogeneity of the small scales:

$$S_3(r) = \left\langle \left[u_L(\mathbf{x}+\mathbf{r}) - u_L(\mathbf{x}) \right]^3 \right\rangle = -\frac{4}{5}\varepsilon r , \quad (2)$$

where ε is the mean rate of energy flux balancing the mean rate of energy dissipation in statistically steady turbulence in the limit of zero viscosity. This so-called "four-fifths law" (Kolmogorov 1941) is a statement of energy conservation in the inertial range; that is, the energy flux through scales of size r_1 equals the energy flux through scales of size r_2 if both r_1 and r_2 are in the inertial range. The four-fifths law is now used as a nominal measure of the regime of inertial-range scaling in experimental and numerical data; that is, the range of scales over which the four-fifths law is close to being satisfied is taken to be the statistically "universal" scaling regime.

Kolmogorov also assumed that the cascade of energy occurs in a space-filling, self-similar way. Formally, there exists a unique scaling exponent h such that

$$S_n(\lambda r) = \lambda^h S_n(r) \quad . \quad (3)$$

To be consistent with the four-fifths law, the assumption of self-similarity implies that $h = 1/3$ and that, in general, if structure functions of arbitrary order are to scale with r, then

$$S_n(r) \approx r^{\zeta_n}, \text{ where } \zeta_n = \frac{n}{3} \quad . \quad (4)$$

Most of the known empirical departures from the Kolmogorov scaling prediction can be traced to three causes: The Reynolds number is not large enough, the scaling is contaminated by the anisotropies inevitable in most flows, and the self-similarity assumption is not valid. The effects relating to small Reynolds numbers are something we have to live with, in a sense, because of the limitations of technology and computational power, but cumulative data analysis of experiments and simulations performed over several decades strongly suggest that the scaling exponents do not differ much for a Taylor microscale Reynolds number[1] R_λ ranging from approximately 100 to approximately 10,000.

It therefore seems that, at a minimum, we observe a convergence of the exponents over a wide range of high Reynolds numbers. The assumption of statistical isotropy, that is, invariance under arbitrary rigid rotations, is key to the scaling-law predictions, but isotropy is a rather strong restriction to make when most turbulent flows are apparently highly anisotropic. There are two ways to remove the inevitable effects of anisotropy in order to test the fundamental assumption of self-similarity. The first is to measure flows with extremely high Reynolds numbers, such as wind flow over the ground, that yield wide separation of scales and resort to the Kolmogorov assumption that, for sufficiently small scales, the statistics will be locally isotropic. The second is to explicitly extract the isotropic component of the statistics, for example, by systematically averaging out the anisotropic contributions, as we discuss in detail below. Recently, the effect of anisotropy on scaling exponents has been studied extensively, and there are now ways to quantify anisotropic effects (Kurien and Sreenivasan 2001), as well as to extract purely isotropic contributions (Taylor et al. 2003), which might then be more sensibly compared with theoretical predictions. We will discuss a new method to implement the latter procedure that has proved to be very useful in analyzing arbitrarily anisotropic flows. The final known reason for departure from the Kolmogorov scaling prediction is that the turbulent cascade is not self-similar. That is, instead of each generation of eddies being produced in a space-filling, self-similar way, the cascade proceeds in an intermittent manner, in which some parts of the flow at a given instant are extremely active while others are relatively quiescent. This is the now well-known intermittency feature of turbulence, and it results in what is known as "anomalous" scaling—that is, there is no unique scaling exponent h from which all scaling exponents can be simply derived.

In the remainder of this article, we describe our studies of the universal statistical features of turbulence using quantities such as the structure functions measured from simulations

[1] The Taylor microscale Reynolds number is $R_\lambda = u'\lambda/\nu$, where u' is the velocity fluctuation and ν is the viscosity. Initially, G. I. Taylor thought that the scale λ—the radius of curvature at the origin of the autocorrelation of the fluctuating velocity—was the viscous dissipation scale of turbulence. In fact, its magnitude is intermediate between the large scale L and the true (Kolmogorov) dissipation scale η. R_λ is often used instead of the large-scale Reynolds number, Re, to characterize flows that have widely varying large-scale properties and, hence, widely varying Reynolds numbers but whose small-scale fluctuations might be comparable. At high Reynolds numbers, $R_\lambda \propto Re^{1/2}$.

(resolved down to the dissipation scale) of the fundamental equations of motion, the Navier-Stokes equations. First, we discuss the simulations themselves and then demonstrate the use of diagnostics to extract statistically isotropic features of the flow. Our results suggest a refinement of the Kolmogorov picture of isotropic turbulence.

Direct Numerical Simulations

Direct numerical simulation (DNS) refers to solving the Navier-Stokes equations numerically by resolving all scales down to the scale of viscous dissipation. DNS represents a brute-force approach to modeling turbulence: No modeling is required beyond the Navier-Stokes equations, simple well-understood numerical methods are used, but massive computing resources are needed. When carefully produced, DNS data is an excellent substitute for exact, analytic solutions of the Navier-Stokes equations. The only drawback is that to obtain solutions for moderately high Reynolds numbers requires weeks of computing time on today's largest supercomputers. To achieve the Reynolds numbers of a typical atmospheric boundary layer flow, $R_\lambda = 10{,}000$, will require a 10^8-fold increase in computing power over today's largest computers. Fortunately, large-scale features such as the mean flow and other statistical properties of turbulence depend only weakly on the Reynolds number. Thus, DNS of flows with more moderate Reynolds numbers has been valuable for studying many aspects of turbulence, including universal statistical features. For additional information, see, for example, the review by Moin and Mahesh (1998).

To obtain as high a Reynolds number as possible, DNS calculations are usually performed on the simplest flows: the incompressible Navier-Stokes equations, without multiple materials or other physics that must be modeled. The calculations are further limited to simple domains and equally spaced grids, which allow for very efficient numerical algorithms. The highest possible Reynolds numbers can be achieved for the classic problem of homogeneous turbulence in a square box with periodic boundary conditions, the problem we have focused on.

For fully resolved calculations, spectral methods are preferred for their high accuracy. Although high-order finite-difference codes can yield similar accuracy, spectral methods still have an advantage because they permit fast, direct solution of Poisson's equation. Solving Poisson's equation is required to determine the pressure gradient that appears in the Navier-Stokes equations. Spectral methods became practical for computational fluid dynamics after the development of the spectral-transform method (Eliasen et al. 1970, Orszag 1970). Additional issues important for the Navier-Stokes equations, such as time-stepping schemes and control of aliasing errors, were effectively treated in Rogallo (1981). The methods used today are quite similar to those used in that work.

The spectral part of a DNS code refers to the method used for the spatial discretization of the equations. In particular, to compute a spatial derivative of a term in the equations, one first expands that term in a truncated Fourier expansion using the fast Fourier transform (FFT) and then computes the derivatives exactly from the Fourier expansion. After the equations are discretized in space, we are left with a system of ordinary differential equations, which are integrated in time with a third- or fourth-order Runge-Kutta or similar scheme. This procedure has one complication arising from the nonlinear advection term. The nonlinearity can transfer energy into frequencies higher than can be resolved by the numerical grid. The energy in these unresolved frequencies will then artificially contaminate the energy and phases of the resolved frequencies in a procedure known as aliasing. This aliasing error is typically controlled by properly designed spectral filters.

The computational expense of DNS comes from the strict restrictions on the grid spacing, Δx, and the time step, Δt, that are required to fully resolve all scales in the Navier-Stokes equations. If one is primarily interested in the statistical properties of the inertial range, it is sufficient to run the numerical simulation with $\Delta x \le 3\eta$, where η is the Kolmogorov length scale.[2]

Since $\eta \sim Re^{-3/4}$ (or $\eta \sim R_\lambda^{-3/2}$), this grid-spacing restriction also determines the highest-Reynolds-number flow that can be accurately computed for a given Δx. The restrictions on Δt can be estimated from the consideration of physical time scales in the problem, but in practice, a more restrictive constraint comes from the CFL (Courant-Friedrichs-Levy) condition, which shows that, for the time-stepping schemes used, the time step must be kept proportional to the grid spacing. Combined, these considerations show that the computational cost of DNS is proportional to R_λ^6 (Pope 2000).

In DNS calculations, it is important to ensure that the energy dissipation is due entirely to the viscous terms in the Navier-Stokes equations, rather

[2] The Kolmogorov length scale η depends only on the rate of energy flux ε and the (chosen) fluid viscosity ν. In the forced simulations, η is determined entirely by the forcing (rate of input of energy), which balances the flux rate in the statistical steady state and the chosen viscosity coefficient. In the decaying simulation, η is fully determined at initial time by the initial condition but thereafter evolves with the dynamics, thus resulting in increasing resolution as the flow decays.

than to the numerical method used. Often, numerical methods are designed to introduce various types of artificial dissipation, which can have beneficial properties but are not appropriate for DNS. For the spectral method outlined here, we estimate the numerical viscosity by computing the kinetic energy E at every time step and comparing the numerical evolution of E,

$$\frac{dE}{dt} = \frac{E(t+\Delta t) - E(t)}{\Delta t} \quad ,$$

where $E = 0.5 \langle \mathbf{u} \cdot \mathbf{u} \rangle$, with the evolution given by the Navier-Stokes equations. In the unforced case, the latter term is

$$\frac{dE}{dt} = -\nu \langle \nabla \mathbf{u} \cdot \nabla \mathbf{u} \rangle \quad ,$$

where $\mathbf{u}$ is the flow field. In our largest simulation, the two quantities agree to more than four digits, demonstrating that over 99.99 percent of the dissipation is due to the Navier-Stokes viscosity.

Finally, if DNS in a periodic box is used to study universal features of turbulence, the largest scales are strongly influenced by the square computational domain. For example, consider a field with all its energy in spherical wave numbers of at most 2. There are only a handful of such Fourier modes, and they are strongly aligned with the coordinate directions of the box. Any such field could not be isotropic. Many of the directional moments of the field would greatly differ between coordinate and noncoordinate directions. There are several ways to avoid this effect in order to obtain more isotropic simulations. The most direct method is to simply keep energy out of the large scales. This is the approach usually taken with decaying turbulence simulations. For forced simulations, it is possible to achieve flows with much higher Reynolds numbers by injecting energy into only the low wave numbers, but to obtain isotropic solutions requires careful attention. One approach is to use stochastic forcing designed so that the flow will be isotropic for a long enough time average, even though the field at any given time will have large anisotropies at the large scales. This approach introduces a lot of fluctuations in the solutions, so long time averages must be taken to obtain converged statistics. The most efficient approach is to use smooth, deterministic low-wave-number forcing. Converged statistics can then be obtained with shorter time averages, but some anisotropy will persist throughout the flow. For many quantities of interest, however, this anisotropy can be removed with the angle-averaging techniques described below.

Table I. Parameters for Five DNS Datasets

Data Set	Grid Points (N)[1]	Forced Flow	R_λ	Duration[2]	Storage per Frame (GB)
1	512	Yes (deterministic)	250	7	3
2	512	Yes (stochastic)	250	12	3
3	512	Yes (deterministic with helicity input)	250	10	3
4	1024	Yes (deterministic)	460	3	24
5	2048	No (initial condition of Johns Hopkins experiment)	170	3	192

[1] N is the number of points on each side of the cubic computational grid.

[2] The duration of a run is measured in units of the large eddy turnover time.

In our work, we have examined DNS simulations for decaying turbulence, stochastically forced turbulence, and deterministically forced turbulence (refer to Table I). For the decaying turbulence simulations, a properly chosen initial condition is allowed to decay through the effects of viscosity. For the forced problems, the simulations are run until the forcing and dissipation reach statistical equilibrium, and then they are run for several additional eddy turnover times to collect data from the equilibrium regime.

The decaying problem has the advantage that more realistic flows can be simulated, and it is possible, in principle, to compare the simulation results with those from experiments, such as those carried out at the recently upgraded Corrsin Wind Tunnel (Kang et al. 2003). But the decaying problem has the drawback that the results strongly depend on the initial condition, and one is faced with the challenge of generating a realistic turbulence state to use for the initial condition. To address this problem, in data set 5, we have followed the procedure described by Kang et al. (2003). We generate an initial flow field with random, uncorrelated phases but a prescribed energy spectrum. The flow is then run for a short time, until the phases become correlated enough to give a reasonable mean-derivative skewness. The energy spectrum is then reinitialized back to the original spectrum while retaining the correlated phases. Our low-wave-number forcing schemes are described in detail in Taylor et al. (2003). The deterministic forcing is based on the work by Sullivan et al. (1994), Sreenivasan et al. (1996), and Overholt and Pope (1998). Data sets 1 and 4 were obtained with this forcing. Data set 3 was obtained with a similar

scheme, but modified to inject helicity into the flow. The stochastic forcing used for data set 2 was based on the forcing given in Gotoh et al. (2002). We used both types of forcing to demonstrate the equivalence of the results when angle averaging is applied to the data.

Parallel Computing Issues

DNS calculations at resolutions of up to 512^3 can now be obtained on moderately large clusters. But the larger DNS calculations currently require Advanced Simulation and Computing (ASC)-class supercomputers. Our largest simulation, with a resolution of 2048^3, requires a 256-fold increase in computing power over that required for a resolution of 512^3. With 8 billion grid points, our 2048^3 simulation is one of the largest ever completed. It required several weeks using 2048 processors of ASC-Q and was made as part of the Laboratory's Science Runs to showcase ASC-Q's performance.

To implement FFT-based DNS codes on distributed memory parallel computers, the community relies almost exclusively on the data-transpose method. Each processor must perform thousands of FFTs per time step, but the data required for those FFTs will be distributed among many other processors. It is quite difficult to write an efficient, distributed-data FFT, and thus the data-transpose method continuously adjusts the distribution of data among the processors so that each processor can use a conventional serial FFT. The name "transpose" comes from the fact that if the data distribution is represented on a 3-D mesh of processors, the operations required by the data-transpose algorithm look like matrix transposes. For a resolution of 2048^3, over a terabyte of data must be moved through the network for each time step, and thus the method relies on a tightly coupled parallel computer with very high bandwidth. On ASC-Q, for problems of size N^3, we obtain excellent scaling for up to $N/2$ processors. Using N processors still represents a significant speedup, but the scalability starts to decrease, so there is little benefit to using more than N processors.

Another important problem concerns data input/output (I/O). For a resolution of 2048^3, each flow snapshot (which can also be used as a restart file) is 192 gigabytes. Serial I/O (having a single processor collect the data from all other processors and write it into a single file) can obtain data rates only in the tens of megabytes per second and thus requires hours to write a single snapshot or read in a snapshot when restarting. To avoid this unacceptable bottleneck, we utilized the Unified Data Model (UDM) I/O library of the High-Performance Computing Environment Group at Los Alamos. UDM, in conjunction with ASC-Q's parallel-file system, allows all processors to participate in the I/O for a single file. With UDM, we were able to obtain data-transfer rates of over 500 megabytes per second, which means snapshots can be written or read in under 7 minutes.

The Angle-Averaging Technique

In general, the two-point structure function $S(r)$ defined in Equation (1) is a function of the vector $\mathbf{r}$, that is, a function of the size of the separation scale $r = |\mathbf{r}|$, as well as of the orientation of $\mathbf{r}$. The Kolmogorov 1941 theory, however, assumes that, for sufficiently small scales, the flow depends only on the magnitude of $\mathbf{r}$ and is independent of the orientation of $\mathbf{r}$. Most reasonably controlled flow experiments (for example, those occurring in wind tunnels or pipes), as well as uncontrolled experiments (for example, those involving measurements of velocity in the atmospheric boundary layer), inevitably have some degree of anisotropy either from boundary configurations or from forcing mechanisms. Therefore, reasonable comparisons with theoretical predictions require understanding the degree of contamination caused by arbitrary anisotropy as well as formulating methods to eliminate these effects from the data. From experiments at very high Reynolds numbers (Taylor Reynolds number of ~10,000 or higher), in which there is wide separation between the large scales and the dissipative scales, we know that, for two-point statistics of the structure functions given in Equation (1), the contamination due to anisotropy decays rapidly with scale size and that local isotropy is recovered in the leading order. In numerical simulations, the Reynolds numbers, as well as the range of scales computed, are much smaller, and anisotropic effects typically do not have enough range of scales to decay sufficiently. As a result, they have a significant contribution in the inertial range. However, the availability of the full spatial and temporal information of the flow field offers other unique possibilities for investigating purely isotropic effects. One general procedure recently developed at Los Alamos is the angle averaging of the structure functions, which averages out the anisotropic contributions of an arbitrary (anisotropic) flow.

The primary motivation for our angle-averaging procedure is the recent derivation of a new version of the Kolmogorov four-fifths law (Duchon and Robert 2000, Eyink 2003). In this version, the four-fifths law states that for any domain B of size R in the limit that the viscosity $\nu \to 0$ (infinite or sufficiently high

Reynolds number), for scales of size $r << R$, and at any instant in time,

$$S_3(r) = \left\langle \left[u_L(\mathbf{x}+\mathbf{r}) - u_L(\mathbf{x}) \right]^3 \right\rangle = \int \frac{d\Omega_r}{4\pi} \int d\mathbf{x} \left[u_L(\mathbf{x}+\mathbf{r}) - u_L(\mathbf{x}) \right]^3 = -\frac{4}{5}\varepsilon_B r \quad , \tag{5}$$

where ε_B is the energy dissipation rate averaged over B. That is, the four-fifths law holds locally, instantaneously, and without any assumption of homogeneity or isotropy. The integration over the solid angle Ω, indicates averaging over all possible orientations of $\mathbf{r}$ for a given $|\mathbf{r}|$, which projects out the isotropic part of the correlation. The statement of energy conservation in the inertial range is now quite different—there is an underlying isotropic component common to all flows that formally obeys the same law that Kolmogorov derived using more restrictive assumptions.

To test this prediction with numerical simulations, we devised a way to take the solid-angle average of the data computed on a grid. The obvious, but computationally expensive and error-prone solution, would be to interpolate the velocity vector field over a sphere of desired radius r and integrate. Instead, we chose to first use the separation vectors allowed by the grid to compute structure functions for a fixed (θ,φ) as a function of r, as follows:

$$S_3(r,\theta,\phi) = \int d\mathbf{x} \left[u_L(\mathbf{x}+\mathbf{r}) - u_L(\mathbf{x}) \right]^3 \quad .$$

Then, we computed a set of these structure functions for various (θ,φ) allowed by our grid so that we have a set of functions $S(r,\theta_1,\varphi_1)$, $S(r,\theta_2,\varphi_2),\ldots$ $S(r,\theta_n,\varphi_n)$ for pairs of angles (θ_i,φ_i) that span the full spherical solid angle rather uniformly. Each S is now a smooth function of r in a particular direction and can be interpolated to obtain $S(r)$ for any r. Then, to yield the angle-averaged value for a particular r, we compute

$$S_3(r) = \frac{1}{n}\sum_{i=1}^{n} w_i S_3(r,\theta_i,\phi_i) \quad . \tag{6}$$

where the weight w_i is the solid angle subtended by the Voronoi cell containing the point $\hat{\mathbf{r}}$.

As $n \to \infty$, the average becomes arbitrarily close to the true spherical integral of Equation (5), and so the isotropic component of the statistics is recovered. The method is not specific to the four-fifths law and can in principle be used to examine the underlying isotropic component of any two-point correlation function, as we demonstrate below.

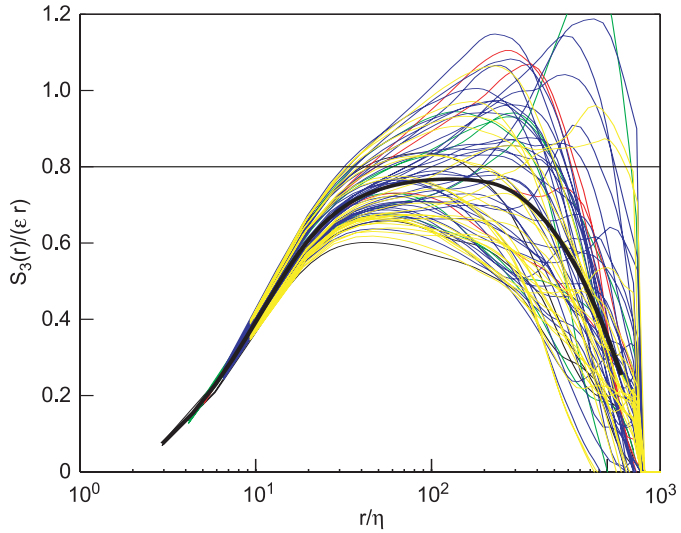

Figure 1. The Four-Fifths Law for a Single Frame of Forced Flow
The four-fifths law was computed for a single frame of data set 4 for deterministic forced flow, whose resolution is 1024^3. Each colored line is the compensated third-order structure function computed in one of 73 different directions of the flow. The black line is the angle-averaged function, which displays a range of scales between 30 and 200 that fall within 5% of the theoretical value of 0.8.

The Four-Fifths Law

Figure 1 shows such a calculation performed on a single frame of an anisotropically forced flow at a resolution of 1024 grid points to a side with periodic boundary conditions (data set 4), which was run long enough to achieve a statistically steady state. Each colored line is the compensated, domain-averaged, longitudinal third-order structure function, $S_3(r)/\varepsilon r$, computed in a particular direction in the periodic box for the increments r allowed by the grid in that direction. The length scale r has been nondimensionalized by the dissipation length scale η. The compensated statistics were computed in 73 different directions that were fairly evenly distributed over the sphere. As is clearly seen, the calculation in a given direction yields a smooth curve, which we interpolated using a cubic spline fit to obtain $S_3(r)/\varepsilon r$ for arbitrary length r in a given direction. The different directions also clearly display a large degree of variability with respect to each other, which appears to diminish as the scales get very small but is significant in a midrange of scales wherein the inertial range might be expected to lie. The thick black line is the average over all 73 directions of $S_3(r)/\varepsilon r$ as a function of r calcu-

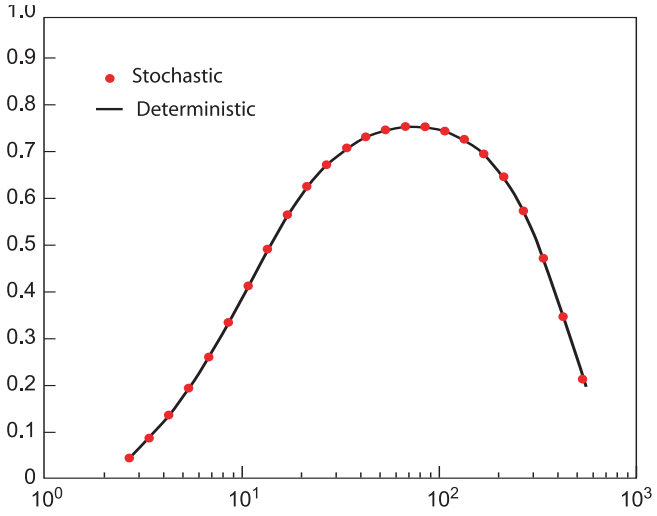

Figure 2. Angle- and Time-Averaged Compensated Third-Order Structure Function for Two Different Forced Flows

The angle- and time-averaged compensated third-order structure function was computed for data sets 1 (solid line) and 2 (dotted line), each of which has a resolution of 512^3. These two differently forced flows essentially coincide with each other in this statistical measure, thus supporting the notion of underlying universality of turbulent flows.

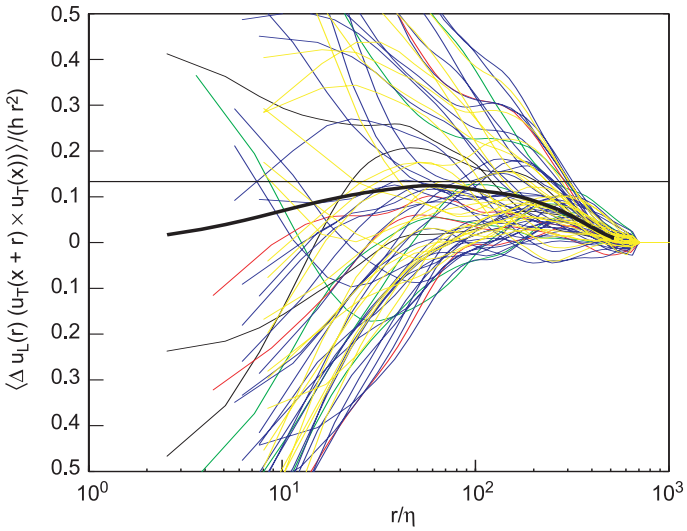

Figure 3. The Two-Fifteenths Law from a Single Frame of Data Set 3

The two-fifteenths law was computed for a single frame of data set 3, whose resolution is 512^3. Each colored line is the compensated third-order statistic in one of 73 different directions in the flow. The black curve is the angle-averaged function, which shows a range between 30 and 200 wherein its value is within 4% of the theoretically predicted value of 2/15.

lated according to Equation (6).

Remarkably, this angle-averaged function displays a reasonable range over which the curve is rather flat (indicating linear scaling in r) and is within 5 percent of 0.8, which is the theoretical predicted value. This result says that, at every instant in an anisotropic flow, there is an underlying isotropic component that can be projected out when an approximated spherical average is used and that, furthermore, obeys to a very good degree the fundamental universal four-fifths law for isotropic flow.

In Figure 2, we show the same calculation for data sets 1 and 2, which were calculated at lower Reynolds numbers but are forced in the low wave numbers as described above. The solid (black) and dotted (red) lines are the angle-averaged and then time-averaged compensated third-order structure functions for data sets 1 and 2, respectively. While the scaling range for this resolution is less than that in Figure 1, the noteworthy feature is that the curves are indistinguishable, which is a strong indication of universality because the underlying isotropic contributions of these two very different anisotropic flows are identical (Taylor et al. 2003).

The Two-Fifteenths Law

To demonstrate the distinction between the Kolmogorov local isotropy assumption and what we see in Figure 1, we discuss the measurement, using the same angle-averaging technique, of a very different statistical quantity that obeys the so-called two-fifteenths law:

$$\left\langle \left[u_L(\mathbf{x}-\mathbf{r})-u_L(\mathbf{x})\right]\left[u_T(\mathbf{x}+\mathbf{r})\times u_T(\mathbf{x})\right]\right\rangle = \frac{2}{15}hr^2 \quad , \quad (7)$$

where h is the mean helicity dissipation rate and u_T denotes the component of $\mathbf{u}(\mathbf{r})$ transverse to $\mathbf{r}$. The quantity on the left side of this equation is a third-order statistic, as is $S_3(r)$ for the four-fifths law, but this new quantity probes the presence of a constant total helicity flux h in the inertial range (Kurien 2003). Like energy, helicity ($\mathbf{u}\cdot\nabla\times\mathbf{u}$) is conserved in turbulence, and our analysis has revealed that in the inertial range, helicity has other conserved properties in common with those of energy, such as constant flux.

Figure 3 shows this parity-breaking third-order statistic normalized by hr^2 in a forced flow in a periodic box of 512 grid points to a side with fixed sign of helicity input into the two lowest modes at each time step (data set 3). The picture in Figure 3 indicates that helicity flux (that is, the appropriate third-order correlation function) is highly anisotropic all the way into the small scales, as shown by the vast spread among the different directions. Nevertheless, there is still

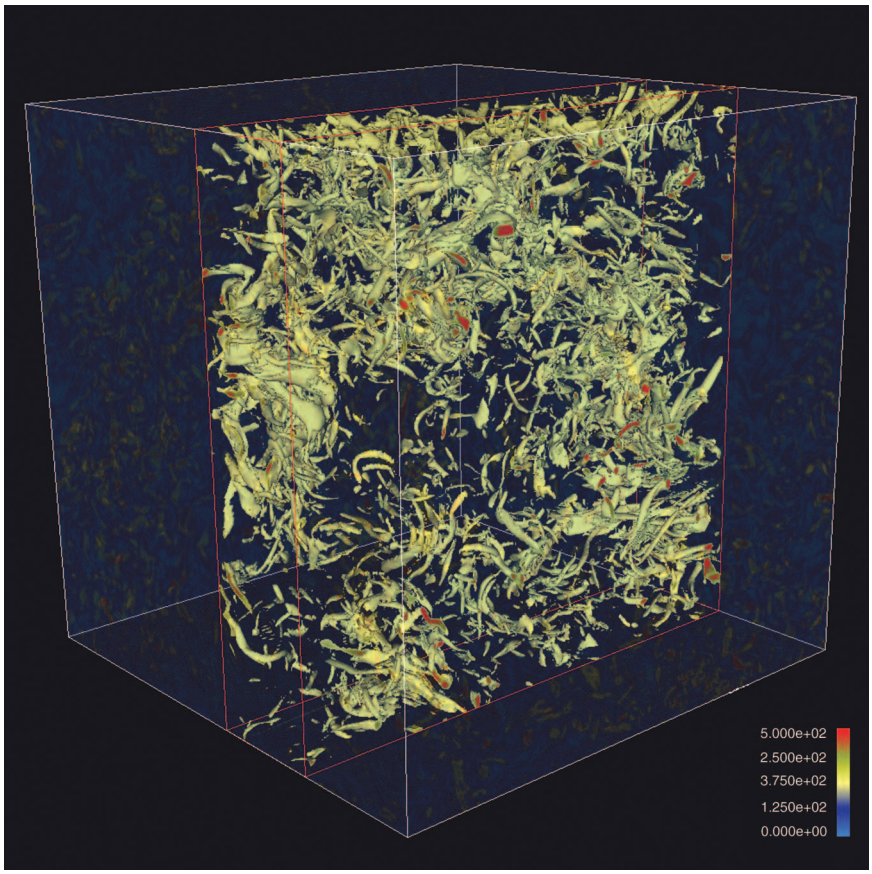

Figure 4. Surfaces of Constant Vorticity for Decaying Turbulence
This visualization is of the surfaces of constant vorticity magnitude in one of the 256^3 subdomains of the entire 2048^3 simulation (data set 5). There are 512 such subdomains in this simulation.

an underlying isotropic component (thick black line) that emerges from the angle-averaging procedure and seems to agree with the universally predicted two-fifteenths law to within 5 percent over a reasonable range of scales. This analysis (Kurien et al. 2004) reveals that the flux of helicity is more anisotropic and intermittent (in the sense of large departures from the mean) than the energy flux measured analogously by the four-fifths law (Figures 1 and 2).

In summary, angle averaging and statistical analysis have revealed that the isotropic component in turbulent flows is universal, agrees rather well with the Kolmogorov theory, and moreover, is consistent with the local version of Duchon and Robert (2000) and Eyink (2003). The procedure allows us to separate the contamination due to anisotropy from other effects, such as small Reynolds number and intermittency, that can muddy the measurement of clean scaling laws. The angle-averaging method also gives us a way to more efficiently use data and gain statistically significant results from single snapshots of the flow, whereas in the past, long time averages were taken, which led to data size and storage issues. Especially when we begin to start looking at the storage and analysis of data set 5, which needs of the order of 250 gigabytes of disk space, a scheme such as the angle-averaging procedure, which increases the amount of information we can glean from a single frame of turbulence data, is a definite asset.

Utility of Large-Scale Simulations

Our largest simulation (data set 5) is for a very highly resolved (2048^3), decaying flow at a moderate Reynolds number (270). The simulation's initial condition was taken from the centerline data gathered from a wind tunnel experiment performed at Johns Hopkins University (Tao et al. 2000). The simulation, performed on 2048 processors of ASC-Q, did not achieve the $R_\lambda \sim 700$ of the experiment. Therefore, direct comparison with the experimental results cannot be made until we can compute decaying flow at a higher Reynolds number or the experimental facility can rerun the experiment at a Reynolds number matching that of the existing simulation. However, a full numerical simulation provides access to the full spatial and temporal velocity field, while the experiments normally measure a sparse subset of the flow field.

Figure 4 shows the surfaces of constant vorticity magnitude for a 256^3 subdomain of the 2048^3 simulation. Vorticity visualizations are typically used to show the locations of the flow structures. In this case, the vorticity visualization shows that the generation of successively smaller energetic structures occurs by the stretching of regions of vorticity by the nonlinearity. The small structures in Figure 4 persist down to the grid size of the simulation.

Data sets 1 and 2 had Reynolds numbers similar to the number for data set 5 but only a quarter of the number of grid points to a side. That is, the linear size of the smallest scales resolved in the 512^3 simulations of data sets 1 and 2 was 64 times larger than the smallest scales in the 2048^3 simulation of data set 5. Because the 512^3 simulations cannot resolve almost two orders

of magnitude in scale that are accessible to the 2048^3 simulation, the coarser simulations obscure the turbulent fine structure seen at higher resolutions. Although they are quite suitable for observing the many inertial-range features described above, the coarser computations obscure the significant energetic events that occur at higher resolution. Clearly if we are to gain a deeper understanding of the spatial and temporal universal properties of turbulence through such numerical calculations, we must continue to pursue ways to compute larger resolved Navier-Stokes simulations and to develop efficient methods for analyzing the enormous quantities of data involved. ■

Further Reading

Duchon, J., and R. Robert. 2000. Inertial Energy Dissipation for Weak Solutions of Incompressible Euler and Navier-Stokes Equations. *Nonlinearity* **13**: 249.

Eliasen, E., B. Machenhauer, and E. Rasmussen. 1970. On a Numerical Method for Integration of the Hydrodynamical Equations with a Spectral Representation of the Horizontal Fields. In *Report No. 2*. Institute for Theoretical Meteorology, University of Copenhagen

Eyink, G. L. 2003. Local 4/5-Law and Energy Dissipation Anomaly in Turbulence. *Nonlinearity* **16**: 137.

Gotoh, T., D. Fukayama, and T. Nakano. 2002. Velocity Field Statistics in Homogenous Steady Turbulence Obtained Using a High-Resolution Direct Numerical Simulation. *Phys. Fluids* **14** (3): 1065.

Kang, H. S., S. Chester, and C. Meneveau. 2003. Decaying Turbulence in an Active-Grid-Generated Flow and Comparisons with Large-Eddy Simulation. *J. Fluid Mech.* **480**: 129.

Kolmogorov, A. N. 1941. The Local Structure of Turbulence in Incompressible Viscous Fluid for Very Large Reynolds Numbers. *Dok. Akad. Nauk. SSSR* **30**: 301.

Kurien, S. 2003. The Reflection-Antisymmetric Counterpart of the Kármán-Howarth Dynamical Equation. *Physica D* **175** (3–4): 167.

Kurien, S., and K. R. Sreenivasan. 2001. Measures of Anisotropy and the Universal Properties of Turbulence. In *New Trends in Turbulence: Turbulence Nouveaux Aspects: École de Physique DES Houches—Ujf and Inpg—Grenoble, a NATO Advanced Study Institute, Les Houches, Session LXXIV, 31 July–September 1, 2000*. p. 53. Edited by M. Lesieur, and F. David. New York: Springer-Verlag.

Kurien, S., M. A. Taylor, and T. Matsumoto. 2004. Isotropic Third-Order Statistics in Turbulence with Helicity: the 2/15-Law. *J. Fluid Mech.* **515**: 87.

Moin, P., and K. Mahesh. 1998. Direct Numerical Simulation: A Tool for Turbulence Research. 1998. *Annu. Rev. Fluid Mech.* **30**: 539.

Orszag, S. A. 1970. Transform Method for the Calculation of Vector-Coupled Sums: Application to the Spectral Form of the Vorticity Equation. *J. Atmos. Sci.* **27** (6): 890.

Overholt, M. R., and S. B. Pope. 1998. A Deterministic Forcing Scheme for Direct Numerical Simulations of Turbulence. *Comp. Fluids* **27** (1): 11.

Pope, S. B. 2000. *Turbulent Flows*. Cambridge, United Kingdom: Cambridge University Press.

Rogallo, R. S. 1981. Numerical Experiments in Homogeneous Turbulence. NASA Technical Report TM81315.

Sreenivasan, K. R., S. I. Vainshtein, R. Bhiladvala, I. San Gil, S. Chen, and N. Cao. 1996. Asymmetry of Velocity Increments in Fully Developed Turbulence and the Scaling of Low-Order Moments. *Phys. Rev. Lett.* **77** (8): 1488.

Sullivan, N. P., S. Mahalingam, and R. M. Kerr. 1994. Deterministic Forcing of Homogeneous, Isotropic Turbulence. *Phys. Fluids* **6** (4): 1612.

Tao, B., J. Katz, and C. Meneveau. 2000. Geometry and Scale Relationships in High Reynolds Number Turbulence Determined from Three-Dimensional Holographic Velocimetry. *Phys. Fluids* **12** (5): 941.

Taylor, M. A., S. Kurien, and G. L. Eyink. 2003. Recovering Isotropic Statistics in Turbulence Simulations: The Kolmogorov 4/5th Law. *Phys. Rev. E* **68** (2): 26310.

For further information, contact Susan Kurien (505) 665-0148 (skurien@lanl.gov) or Mark Taylor (505) 284-1874 (mataylo@sandia.gov).